A series of lead(II)/iodine hybrid polymers based on 1-D and 2-D metal–organic motifs linked by different organic conjugated ligands†

Yun Jie Wang,[a] Hao Hong Li,[a] Zhi Rong Chen,*[a] Chang Cang Huang,[a] Xi He Huang,[a] Miao Feng[b] and Yun Lin[c]

The introduction of series of organic conjugated ligands into the Pb/I system leads to the formation of three lead(II)/iodine polymers [Pb$_2$I$_4$(dpdo)]$_n$ (**1**) (dpdo = 4,4′-dipyrdiyl-*N,N*′-dioxide), [PbI$_2$(bipyO$_2$)]$_n$ (**2**) (bipyO$_2$ = 2,2′-dipyrdiyl- *N,N*′-dioxide) and {[PbI(Dhydql)]·DMF}$_n$ (**3**) (Dhydql = deprotonated 8-hydroxyquinoline). In **1** and **2**, both the organic and inorganic ligands are neutral. But the organic moiety in **3** is a conjugated negative ion and the inorganic component presents a 2-D layer arrangement. The organic ligands in this work serve as bridges to link the inorganic chain or layer to heighten the structural dimension. As expected, based on the bridge nature of an organic ligand, **1** features a 2-D arrangement of a staircase-like lattice sheet [Pb$_2$I$_4$(dpdo)]$_n$, **2** exhibits a 1-D chain [PbI$_2$(bipyO$_2$)]$_n$ consisting of unprecedented twisted boat from seven-membered rings, and **3** presents a host–guest structure with DMF as guest molecules which are embedded in between adjoining inorganic–organic components. Furthermore, the compounds were further characterized with fluorescence, UV-vis spectra and third-order non-liner optical (NLO) properties.

Introduction

Currently, considerable attention is focused on fundamental as well as more applied studies of Pb(II)/I hybrid materials owing to their substantial potential application, *e.g.*, electrical, magnetic, optical, transport, nonlinear optical response, and other physical properties.[1–17] Pb/I coordination polymers are attractive targets for crystal design since two aspects are controllable: the organic counter cations and linking ligand units.[18] Compared with the first component, the second one has a direct and better impact on the structure and functionality of a polymer. For this reason, the incorporation of linking ligands into a lead(II)/iodide framework to modify the structure–properties relationship with the aim of yielding functional materials with novel properties, represents a significant studying direction in the materials design field. So far, Pb/I coordination polymers with different dimensions linked by organic bridge ligands have been well established.[19–24] These compounds are generally characterized by PbI$_6$ octahedra with common faces, edges, or vertices. However to our knowledge, most of the previous works only use un-conjugated organic ligands, such as aliphatic amines, whereas hybrid Pb/I systems constructed of conjugated ligands are still rare.[23,24] As we all know, the aliphatic bridges could hinder the free electron transfer among inorganic moieties, which is inhibiting functional properties, but the conjugated ligand promotes the electron flowing among the hybrid framework. In

view of this, we focus our attention on the introduction of organic conjugated ligands to construct the hybrid framework, and we aim to provide a deeper insight into the influence of organic conjugated ligands on the structure and properties of Pb/I inorganic–organic hybrid polymers. In the present work, we adopt the heterocyclic organic molecules to serve as bridge ligands, and furthermore, in order to obtain electron transfer in a longer range, we use the oxidized bipyridine(Scheme 1) in which a larger spacer is involved. We look forward to the birth of novel properties, especially the semiconductor, fluorescence and third-order non-liner optical (NLO) properties. Herein, we describe the synthesis, crystal structures and some properties of three lead(II)/iodine polymers: [Pb$_2$I$_4$(dpdo)]$_n$ (**1**), [PbI$_2$(bipyO$_2$)]$_n$ (**2**) and {[PbI(Dhydql)]·DMF}$_n$ (**3**).

Results and discussion

Structure analyses

Compounds 1, 2. In compounds **1** and **2**, we use two neutral conjugated molecules as bridge ligands to react with Pb(NO$_3$)$_2$ and NaI·2H$_2$O and, as expected, two hybrid compounds constructed from Pb/I inorganic coordination moieties with a linkage of organic bridged ligands were obtained. According to structural analysis, **1** and **2** contain two types of 1D inorganic chains: [Pb$_2$I$_4$O$_2$]$_n$ (**1**) double chains and [PbI$_2$O$_2$]$_n$ (**2**) single chain, respectively. Besides, supramolecular interactions based
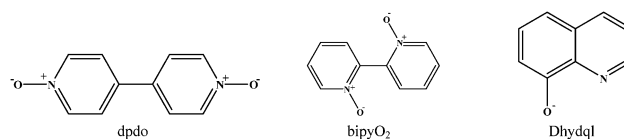
[a]College of Chemistry and Chemical Engineering, Fuzhou University, Fuzhou, Fujian, 350002, China
[b]College of Materials Science and Engineering, Fuzhou University, Fuzhou, Fujian, 350002, China
[c]Instrumental Measurement and Analysis Center, Fuzhou University, Fuzhou, Fujian, 350002, China
† CCDC reference numbers 634298–659647. For crystallographic data in CIF or other electronic format see DOI: 10.1039/b718905b
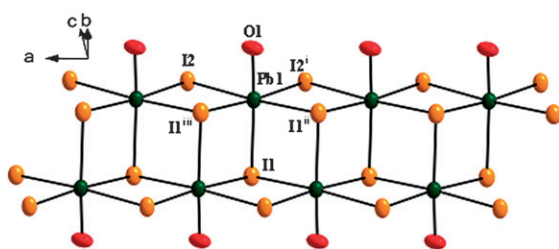

Scheme 1

Fig. 1 View of the 1-D chain in **1** with the red–yellow–blue color representing the $[Pb_2I_4O_2]_n$ chain. Symmetry codes: (i) $1 + x, y, z$; (ii) $1 - x, 2 - y, 1 - z$; (iii) $-x, 2 - y, 1 - z$.

on C–H···I hydrogen bonds were observed between inorganic–organic components.

The molecule in compound **1** is asymmetric, crystallized in a triclinic system with a space group $P\bar{1}$. The inorganic part is $[Pb_2I_4O_2]_n$ as double chains (Fig. 1) and the organic moiety is 4,4′-dipyrdiyl-N,N'-dioxide (dpdo). The inorganic and organic components are linked together through terminal oxygen atoms of dpdo to give a 2-D inorganic–organic staircase-like lattice sheets $[Pb_2I_4(dpdo)]_n$ (Fig. 2).

In **1**, there is only one crystallographically independent lead(II) atom, and two types of iodine atoms defined by their connectivity to Pb: μ_2-I (I2) and μ_3-I (I1). All lead atoms are six-coordinated by one oxygen atom from the bridged ligand and five iodine atoms to give distorted PbI_5O octahedron. These distorted PbI_5O octahedra are further linked by μ_3-I(I1) to form $Pb_2I_8O_2$ bioctahedra, which are *cis*-edge-shared with adjacent $Pb_2I_8O_2$ bioctahedra to present an 1-D double chain $[Pb_2I_4O_2]_n$ along the crystallographic a axis. To the best of our knowledge, such a double-chain structure is rare and only one similar chain was found in compound $Pb_2I_4[L]$ (L = N,N'-bis(3-pyridyl methyl)-1,4-biphenylene dimethyleneimine).[22] Structural analysis reveals that the bond lengths of μ_3–I–Pb in compound **1** are 3.23(5), 3.28(6) and 3.39(3) Å, respectively; likewise, the distances of μ_2–I–Pb are also different, 3.13(5) and 3.21(5) Å, respectively; all of the bond distances being shorter than those in compound $Pb_2I_4[L]$. The Pb–O bonds length is 2.36(2) Å, shorter than that in compound $PbI_2Cu(BSPA)_2$.[25] The I–Pb–I, I–Pb–O angles of diagonal were nearly linear [174.45(3)–176.43(2)°], and the *cis*-I–Pb–I angles are almost upright in the range of 82.84(25) to 93.65(3)°, deviating from the ideal values (90 and 180°) for an octahedron.

In compound **1**, the neutral conjugated bidentate ligand uses its two terminal O atoms as coordination points to realize extending of the structure, and they adopt the same conformation as that in compound $Pb_2I_4[L]$. In other words, the inorganic double chains are linked together through terminal oxygen atoms of dpdo to give a 2-D inorganic–organic staircase-like lattice sheets $[Pb_2I_4(dpdo)]_n$ along the bc plane. According to crystallographic data, the 4,4′-bipyridyl ligand lies at about an inversion center. From this sample structure (Fig. 2a), we found that two pyridine rings of 4,4′-bipyridine N,N'-dioxide ligand are essentially coplanar, and all the adjacent organic bridges are parallel. The centroid–centroid distance between the parallel 4,4′-bipyridine rings is 4.50 Å, which is smaller than that in compound $Pb_2I_4[L]$ (4.65Å). Also, the distance between the nearest inorganic components is 12.0 Å, hence the size of the inorganic–organic lattice is *ca.* 4.5×12.0 Å^2 (Fig. 2a).

Taking the van der Waals radii of H and I to be 1.20 and 2.15 Å, respectively, any H···I contact less than 3.35 Å and C–H···I angle >130° may therefore be potentially considered as significant.[26a] In addition, Batsanov also put forward a set of van der Waals radii with the H and I values of 1.2 and 2.1 Å. According to the above radii values, the H···I distances, being shorter than 3.3 Å, could be treated as hydrogen bond interaction.[26b] In **1**, these discrete 2-D staircase-like lattice sheets $[Pb_2I_4(dpdo)]_n$ are further packed together by intermolecular hydrogen bonds of C–H···I (Fig. 4a). As shown in Fig. 4a, the hydrogen atoms linking with C1 and C5 involves the hydrogen bond interactions with iodide atoms of the neighboring sheets. And two kinds of hydrogen bonds are observed due to their difference in the bond length and angle. The detailed hydrogen bond parameters are as follows: for C1–H1···I2[vi] H-bond, H1···I2[vi] distance: 3.23 Å (vi: $-x, 2 - y, -z$), C1–H1···I2[vi] angle: 132°, for C5–H5···I1[vii] H-bond, H5···I1[vii] distance: 3.27 Å, C5–H5···I1[vii] angle: 133°(vii:$-x, 2 - y, -z$). The C1–H1···I2[vi] hydrogen bond with a bond length of 3.23 Å is somewhat stronger than the C5–H5···I1[vii] one (3.27 Å). The importance of such C–H···I interactions in the supramolecular self-assembly has also been reported.[26a, 27]

The structure of compound **2** consists of an unprecedented 1-D infinite inorganic chain $[PbO_2I_2]_n$, which can be described as the *trans*-edge sharing of PbI_4O_2 octahedron along the c axis (Fig. 3). Pb1 is located on a twofold axis, is six-coordinated and lies in a very distorted octahedron environment, bonding to two pairs of bridging iodine ligands and to one pair of oxygen atoms of the chelating bipyO$_2$ ligand. The Pb–O bonded distance
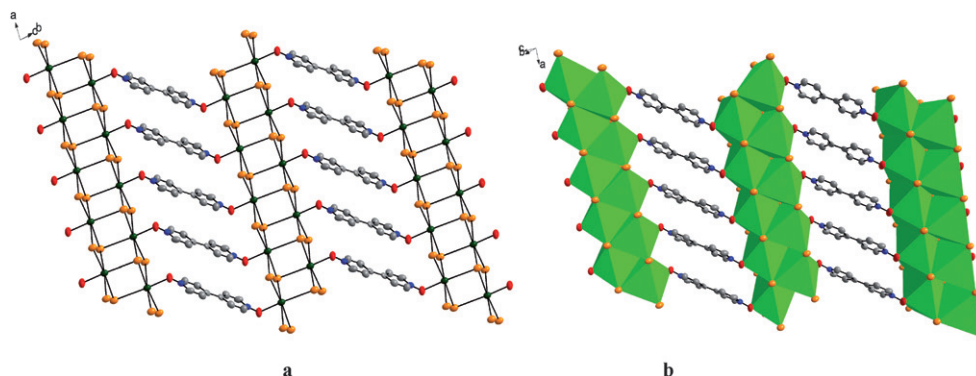

Fig. 2 View of the 2-D "stair-like" sheet (a) and lead(II) octahedra geometry (b) in compound **1**, with hydrogen atoms being omitted for clarity.

is in agreement with the strong Pb–O bond 2.37(1) Å, slightly longer than those in **1** but shorter than in compounds PbI$_2$Cu$_2$(BSPA)[25] and Pb$_2$I$_4$ Cu$_2$ (DMAE)$_4$(DMSO).[28] The observed Pb–I distances are 3.21(6) and 3.48(2) Å, lying in the range of intermediate and weak bonds.[29] Besides, the O–Pb–O bond angle is 73.9°. The *cis*-O–Pb–I and *trans*-O–Pb–I bond angles range from 79.20 to 89.59° and from 152.52 to 153.50°; likewise, *cis*-I–Pb–I and *trans*-I–Pb–I bond angles are 84.20–100.36° and 127.63–169.52°, respectively, indicating that the PbI$_4$O$_2$ octahedron exhibits more apparent distortion than that of the PbI$_5$O octahedron in **1**.
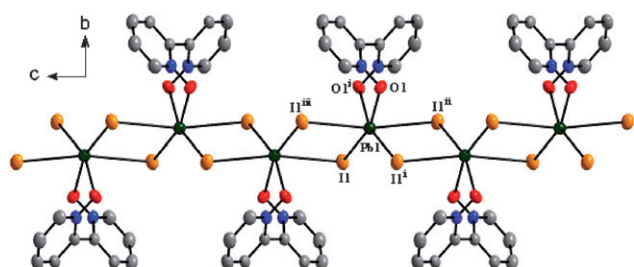
Fig. 3 View of the 1-D inorganic–organic chains in compounds **2**, with hydrogen atoms omitted for clarity.

Similar to compound **1**, the inorganic and organic components in **2** are linked through organic (O) atoms to form 1-D inorganic–organic chains. The bipyO$_2$ units lie on the alternate sides of each chain, which runs parallel to the *c*-axis, respectively. Compared with **1**, a strikingly different feature of **2** is that the two aromatic rings of the organic ligand are not coplanar. The dihedral angle between the two pyridine rings in bipyO$_2$ is *ca.* 49.98°. The adjoining 1-D inorganic–organic chains of compounds **2** are also further linked by a weak C–H⋯I hydrogen bond (Fig. 4b) (H-bond parameters: C2–H2⋯I1^{iv}, H2⋯I1^{iv} distance: 3.24 Å, angle: 139°, iv: 0.5 + *x*, 0.5 − *y*, 0.5 + *z*).

Compound 3. Different from compounds **1** and **2**, compound **3** with a negative ion chelating agent is typical of the 2-D [PbION]$_n$ layer with monoclinic unit cells. In **3**, DMF as guest molecules are embedded in between adjoining inorganic–organic [PbI(D-hydql)] sheets to form a 2-D alternated host–guest inorganic–organic layered structure.

Lead(II) atoms are also six-coordinated and lie in a more distorted octahedron environment, and the inorganic moiety is 2the -D layer which is built up from a characteristic corner-sharing PbI$_3$O$_2$N octahedron (Fig. 5a). In the PbI$_3$O$_2$N octahedron, the lead(II) center coordinates to two oxygen atoms,
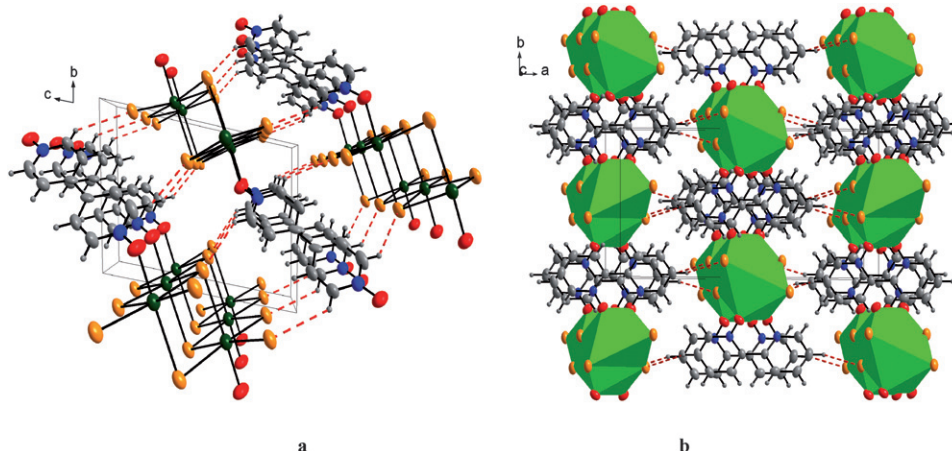
Fig. 4 Packing sketch based on the hydrogen bond supermolecular interactions of compounds **1** (a) and **2** (b).

Fig. 5 (a) The connection mode of Pb and the C–H⋯O hydrogen bond in compound **3**. Symmetry codes: (i) −*x*, 1 − *y*, 1 − *z*; (ii) −*x*, 2 − *y*, 1 − *z*; (iii) *x*, 1.5 − *y*, 0.5 + *z*; (iv) −*x*, −0.5 + *y*, 1.5 − *z*. (b) View of the 2-D inorganic layer of compound **3**, the Pb–Pb interaction is shown in dashed lines.

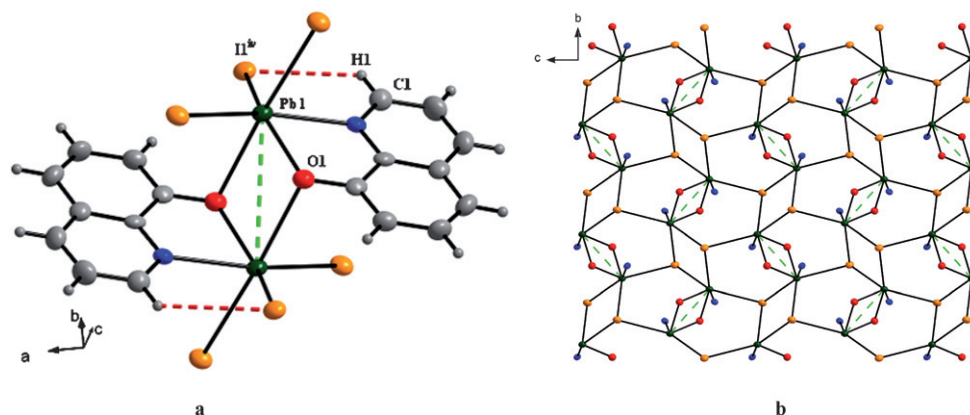one nitrogen atom from $(C_9H_6NO)^-$ anions and three iodine atoms. In the PbI_3O_2N octahedron, I1 occupies the axial direction position, $I1^{ii}$ and $I1^{iii}$ are located at the equator plane. The adjoining PbI_3O_2N octahedra are *cis*-edge-sharing (I–I, O–O) and vertex-sharing (I) to give a unique 2-D layer along the *bc* plane (Fig. 5b).

In the direction parallel to the layers, the cohesion is achieved by strong ionic bonds between equatorial iodide and lead atoms. The coordination geometry of the Pb/I framework shows an axial compression of the octahedral geometry, with the equator $Pb1–I1^{ii}$ and $Pb1–I1^{iii}$ distances [3.519(4) Å and 3.604(6) Å, respectively] longer than the axial Pb1–I1 distance [3.203(1) Å]. The equator Pb–O and Pb–N bond distances are 2.294(6) and 2.476(5) Å, respectively. However the axial Pb–O bond distance is 2.586(4) Å, which is longer than that in compounds **1**, **2** and in $PbI_2Cu_2(BSPA)$,[25] $Pb_2I_4Cu_2$ $(DMAE)_4(DMSO)_2$.[29] The *cis*-angles [from 69.39(14) to 110.78(1)°] between the related lead(II), iodine, oxygen, nitrogen atoms have an apparent deviation from 90°. All *trans* angles [ranging from 133.41(1) to 159.57(8)°] deviate from 180° because of the centre of inversion. The distance between two lead(II) atoms located in a diagonal position in the parallelogram (Pb–O–Pb–O parallelogram, Fig. 5a) is *ca.* 3.95 Å, which shows that there is a weak Pb⋯Pb interaction.

The $(C_9H_6NO)^-$ ions occupy an opposing position and ordered along the inorganic layer (Fig. 6). Each lead atom is chelated by $(C_9H_6NO)^-$ anion to form a five-member ring (N–O–C–C–Pb). And all of the atoms in the ring are essentially coplanar with an rms deviation from the five-member ring mean plane of 0.0476 Å. The ring is slightly tilted to the inorganic layer. In the direction perpendicular to the inorganic layers, the crystal cohesion is achieved by $C1–H1⋯I1^{iv}$ (iv: $-x$, $-0.5 + y$, $1.5 - z$) hydrogen bridge (Fig. 5a), the H1⋯I1 bond distance and $C1–H1⋯I1^{iv}$ bond angle are 3.15 Å and 135°, respectively.

Recently, the hybrids templated with bifunctional ammonium cations, for example, (hydroxyethyl) ammonium $[(HO(CH_2)_2NH_3)]^+$,[30] aminocarboxylic acid $[HO_2CCH_2NH_3]^+$[31] cations and an organic anionic–cationic co-template

$[(H_2en)_7(C_2O_4)_2]^{10+}$,[32] have been reported. In addition, Mitzi *et al.*[33] have described the intercalation of neutral solvent molecules into the organic cation perovskite inorganic–organic hybrid. In total, the templates in all of these hybrids are limited to organic cations, sole organic anions have never been included in hybrid structures, probably because their negative charge is thought to repel inorganic components and would thus make these structure unstable. So, in the traditional opinion, it's too difficult for sole organic anions to be included in Pb/I hybrid structures. However, according to our study, it is found that organic anions can also be introduced into the Pb/I system through controlling the reaction conditions, such as pH value, the ratio of Pb/I/anions, reaction temperature, *etc.*

Fluorescence emission spectrum

Luminescence spectra for solid compounds **1–3** show that there is significant shift in emission spectra. Details of this fluorescence experimentation for compounds **1–3** are listed in Table 1 (Fig. 7). Compound **1** shows a strong emission peak at 582 nm when it is excited at 347 or 401 nm. It exhibits a 62 nm red shift compared with the emission spectrum for $[PbI_2(4,4'$-bipyridine)].[34] Compound **2** presents an emission peak at 514 nm when being excited at 399 nm. A 69 nm blue shift compared with the emission spectrum for $[PbI_2(2,2'$-bipyridine)]$_n$[23] could be observed. A probable reason is that two aromatic rings in the $bipyO_2$ ligand are non-coplanar, which lowers the conjugacy compared with 2,2-bipy. Compound **3** exhibits a weak photo-luminescent emission band at 593 nm and relatively weaker photoluminescent emission shoulder peaks at 475 nm upon photoexcitation at 386 nm. Generally speaking, the observed luminescence could be attributed to any one of the transitions: ligand-centred, metal-centred, or charge transfer in character. The metal–ligand charge-transfer transitions could be observed

Table 1 Details about fluorescence experimentation for the studied compounds

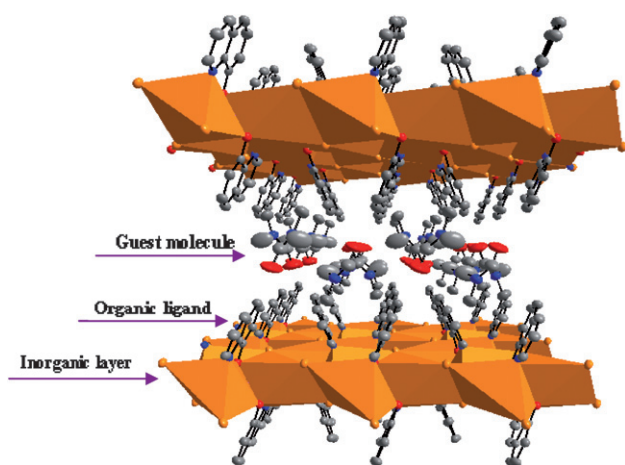| Compound	$\lambda_{em}/\lambda_{ex}$/nm	Intensity
$[Pb_2I_4(dpdo)]_n$ (**1**)	582/347,401	3.75/ 1.25, 1.75 ($\times10^4$)
$[PbI_2(bipyO_2)]_n$ (**2**)	514/399	1.375/ 3.4 ($\times10^4$)
$[(PbI\cdot Dhydql)\cdot DMF]_n$ (**3**)	592,475/436,386	1.5, 0.5/4.32, 4.6 ($\times10^3$)

Fig. 6 A packing sketch of compound **3** down *c* axis. DMF as guest molecules are embedded between two adjoining inorganic–organic [PbI(Dhydql)] sheets. Hydrogen atoms were omitted for clarity.
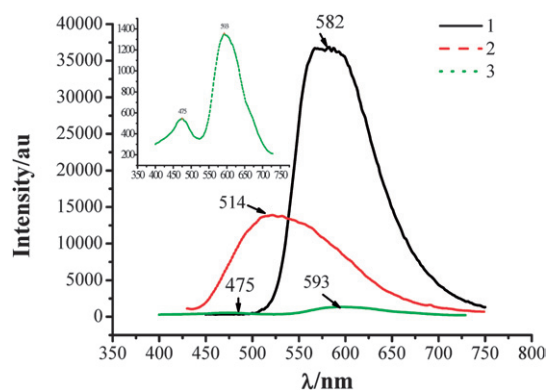

Fig. 7 Solid-state emission spectrum of the studied compounds at room temperature.

at lower wavelength at about 300–400 nm. So for compounds **1–3**, the emission fluorescence might be assigned to the possibility that the metal-centred process involves more than one metal center, which is consistent with statements given in literature.[32,35,36] Also, we can't rule out the possibility that the Pb–I bond is a source of emission. Practically, 8-hydroxyquinoline has no fluorescence property,[37] but the non-rigid plane becomes rigid when it chelated with Pb^{2+}, which is in favor of π-electron cloud superposition and made the structure of the rigid plane more stabilized. When the molecules go back to a ground state from an excited state, the probability of radiationless transition decreases greatly, therefore it shows fluorescence emission.

Optical properties

The diffuse-reflectance spectra of PbI_2 and compounds **1–3** have been measured at room temperature and plotted in Fig. 8 as a $F(R)^2$ vs photon energy diagram according to the Kubelka–Munk function.[38–40] Their optical band gaps (E_g) determined by the extrapolation method[41,42] are 2.50, 2.82 and 2.75 eV for compounds **1–3**, respectively, suggesting that the present compounds belong to semiconductors (Fig. 8). The experimental
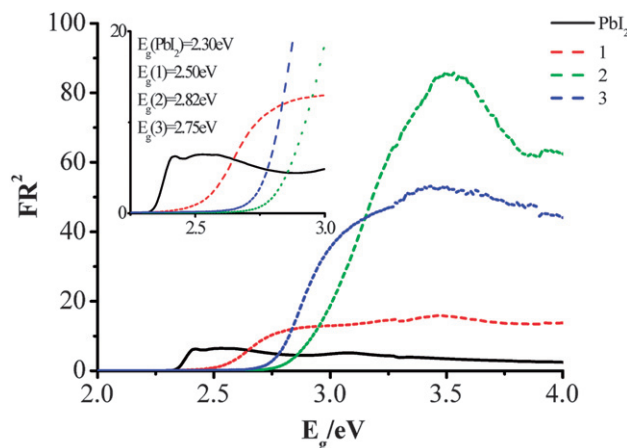
values exhibit a 0.2–0.52 eV blue shift of the absorption edges compared with the measured value of 2.30 eV for bulk PbI_2.

Third-order non-linear optical (NLO) property

The third-order NLO properties of compounds **1** and **2** were investigated with pulses of a wavelength of 532 nm, a duration of 8 ns and the energy of illumination 2×10^{-4} J by a Z-scan experiment using an open-aperture configuration with 1.0×10^{-4} mol L^{-1} in DMF solution. Fig. 9 depicts the NLO absorption properties of **1** and **2**, which clearly illustrates that the absorption increases as the intensity of the incident light rises, with light transmittance (T) being a function of the Z position of the samples.[43] A reasonably good fit between the experimental data and the theoretical curves[43,44] was obtained. It is clear that the theoretical curves qualitatively reproduce the general pattern of the observed experimental data. This result suggests that the experimentally detected NLO effects have an effective third-order characteristics. The effective nonlinear absorptive index β is derived to be 2.678×10^{-14} cm W^{-1} (1) and 4.495×10^{-14} cm W^{-1} (2), respectively.

Summary

This paper reports the synthesis and properties of three kinds of organic–inorganic hybrid materials based on PbI_2 and a series of organic conjugated ligands. Our work in this paper has demonstrated the phenomenon that the introduction of new organic conjugated ligands always leads to a dramatic structural change of the basic inorganic phases. With regard to **1** and **2**, the stereospecific blockade of these ligands has an important effect on the linkage modes of PbI_aO_b ($a + b = 6$) octahedron, resulting in different types of a chain-like structure $[Pb_2I_4O_2]_n$ and $[PbI_4O_2]_n$. It also seems that the structure of the inorganic moiety becomes more simple when the stereospecific blockade increases. However in compound **3**, the oxygen anions can attract more Pb^{2+} cations around them, and as a result, the Pb/I framework will have to increase its positive charge in order to satisfy the neutrality requirement and may thus yield new types of 2-D layer structures in hybrids. Up to now, in the case of iodoplumbates, the chain $[Pb_2I_4O_2]_n$[45] and $[PbI_4N_2]_n$[23] have been reported, but

Fig. 8 Optical absorption spectra for **1–3** and PbI_2.
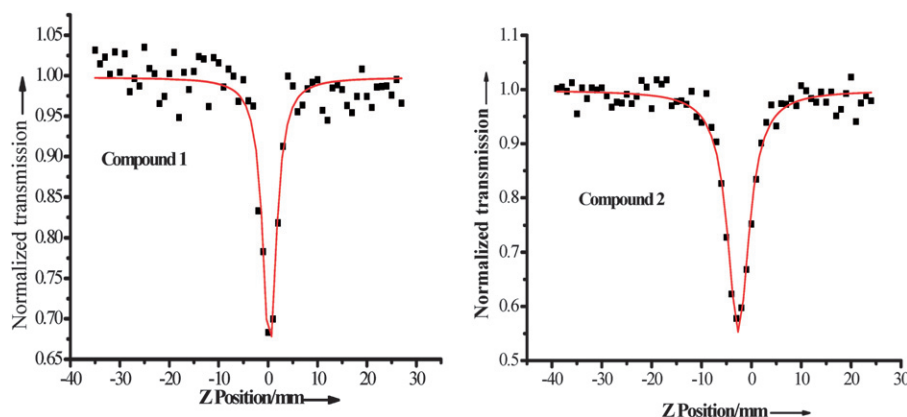
Fig. 9 Z-Scan data for compounds **1** and **2** in *ca.* 1.0×10^{-4} mol dm^{-3} DMF solution, obtained under an open aperture configuration. The block squares are the experimental data, and the solid curve is the theoretical fit.

Table 2 Crystal data and structure refinement summary for the compounds studied

	1	2	3
Formula	$C_5H_4I_2NOPb$	$C_{10}H_8I_2N_2O_2Pb$	$C_{12}H_{13}IN_2O_2Pb$
Formula weight	555.09	649.18	551.34
T/K	293(2)	293(2)	293(2)
Crystal system	Triclinic	Monoclinic	Monoclinic
Space group	$P\bar{1}$	$C2/c$	$P2_1/c$
Z	2	4	4
a/Å	4.5644(9)	18.866(4)	16.872(5)
b/Å	8.9738(9)	8.6033(7)	7.2993(17)
c/Å	11.778(2)	9.6102(9)	12.074(3)
α/°	78.05(3)	90.00	90.00
β/°	83.67(3)	115.43(3)	107.850(4)
γ/°	84.67(3)	90.00	90.00
Cell volume/Å³	467.88(16)	1408.7(5)	1415.4(6)
Limiting indices	$-5 \le h \le 5$, $-11 \le k \le 11$, $-15 \le l \le 15$	$-24 \le h \le 24$, $-11 \le k \le 11$, $-12 \le l \le 12$	$-21 \le h \le 21$, $-9 \le k \le 9$, $-15 \le l \le 15$
μ/mm⁻¹	24.567	16.351	14.096
D_{calc}/Mg m⁻³	3.940	3.061	2.587
Reflections collected	4670	6759	10536
Independent reflections	2140	1629	3253
Reflections observed	1510	1495	2863
$F(000)$	474.0	1144	1000.0
Final R indices $(I > 2\sigma(I))^a$	$R_1 = 0.0511$, $wR_2 = 0.0997$	$R_1 = 0.0308$, $wR_2 = 0.0641$	$R_1 = 0.0331$, $wR_2 = 0.0735$
R indices (all data)	$R_1 = 0.0736$, $wR_2 = 0.1108$	$R_1 = 0.0345$, $wR_2 = 0.0655$	$R_1 = 0.0377$, $wR_2 = 0.0760$
S	0.949	1.071	1.025
$\triangle\rho_{max}$/e Å⁻³	2.447	0.881	2.335
$\triangle\rho_{min}$/e Å⁻³	-1.900	-0.979	-2.525

^{a} $R_1 = ||F_0| - |F_C||/|F_0|$, $wR_2 = [w(F_2^0F_2^C)^2/[w(F_0^2)^2]^{1/2}$.

the $[PbI_4O_2]_n$ chain and the $[PbINO]_n$ 2-D layer structures are a new Pb/I organic structural arrangement.

Experimental

Characterization

$BipyO_2$ was prepared as reported in literature.[47] Other chemicals were of reagent grade quality obtained from commercial sources and used without further purification. C, H, N analyses were carried out with a Vario EL III element analyzer. IR spectra were recorded on a Nicolet Co. Magna-IR 750 spectrometer with KBr pellets in the 4000–400 cm⁻¹ regions. Optical diffuse reflectance spectra were measured on a PE Lambda 35 UV-vis spectrophotometer equipped with an integrating sphere at 293 K, and a $BaSO_4$ plate was used as reference. The values of E_g were obtained with the use of a straightforward extrapolation method.[46] Fluorescence spectra were carried out on a PW2424 spectrometer. The third-order non-liner optical (NLO) properties of compounds **1** and **2** were investigated by pulses of a wavelength of 532 nm, a duration of 8 ns and an intensity of the illumination 2×10^{-4} J by a Z-scan experiment.

Synthesis of compounds

$[Pb_2I_4(dpdo)]_n$ (1). **1** was synthesized by self-assembling reactions of $Pb(NO_3)_2$, $NaI \cdot 2 H_2O$ and dpdo in DMF solvent. Dpdo (0.19 g, 1.0 mmol), $Pb(NO_3)_2$ (0.66 g, 2 mmol) were dissolved in 15 mL DMF and stirred for 20 min, and then $NaI \cdot 2 H_2O$ (0.64 g.4 mmol) was added into the above solution with the pH value being adjusted to 5.0 by an addition of 10% HNO_3/DMF solution. The mixed solution was stirred for

Table 3 Selected bond lengths (Å) and bond angles (°)

Compound 1

Pb1–O1	2.35(2)	Pb1–I1ⁱⁱ	3.23(5)	I1–Pb1ⁱⁱ	3.28(6)
Pb1–I2ⁱ	3.13(6)	Pb1–I1ⁱⁱⁱ	3.28(6)	I1–Pb1ⁱⁱⁱ	3.28(6)
Pb1–I2	3.21(5)	Pb1–I1	3.39(3)	I2–Pb1ⁱᵛ	3.13 (6)
O1–Pb1–I2ⁱ	92.13(24)	I2ⁱ–Pb1–I1ⁱⁱ	90.27(2)	I1ⁱⁱ–Pb1–I1ⁱⁱⁱ	89.16(2)
O1–Pb1–I2	86.64(24)	I2–Pb1–I1ⁱⁱ	174.45(3)	I1ⁱⁱⁱ–Pb1–I1	93.67(2)
O1–Pb1–I1	176.51(27)	I2ⁱ–Pb1–I1ⁱⁱⁱ	175.03(3)	Pb1ⁱⁱ–I1–Pb1ⁱⁱⁱ	89.16(2)
O1–Pb1–I1ⁱⁱ	88.24(24)	I2–Pb1–I1ⁱⁱⁱ	88.09(2)	Pb1ⁱⁱ–I1–Pb1	87.51(2)
O1–Pb1–I1ⁱⁱⁱ	82.92(24)	I2ⁱ–Pb1–I2	92.06(2)	Pb1ⁱⁱⁱ–I1–Pb1	86.33(2)
I2ⁱ–Pb1–I1	91.29(2)	I1ⁱⁱ–Pb1–I1	92.49(3)	Pb1ⁱᵛ–I2–Pb1	92.06(2)
I2–Pb1–I1	92.49(2)				

Compound 2

Pb1–O1	2.37(1)	Pb1–O1ⁱ	2.37(1)	Pb1–I1ⁱⁱ	3.21(6)
Pb1–I1ⁱ	3.48 (2)	Pb1–I1	3.48(2)	I1–Pb1ⁱⁱⁱ	3.21(6)
O1–Pb1–O1ⁱ	74.05(5)	I1ⁱⁱ–Pb1–I1ⁱⁱⁱ	169.52(1)	O1–Pb1–I1	153.11(2)
O1ⁱ–Pb1–I1ⁱⁱⁱ	82.26(11)	I1ⁱⁱⁱ–Pb1–I1ⁱ	100.36(1)	I1ⁱ–Pb1–I1	127.63(1)
I1ⁱⁱ–Pb1–I1ⁱ	84.30(1)	I1ⁱⁱⁱ–Pb1–I1	84.30(1)	O1–Pb1–I1ⁱⁱⁱ	89.35(11)
I1ⁱⁱ–Pb1–I1	100.36(1)	O1ⁱ–Pb1–I1ⁱⁱ	89.35(11)	O1ⁱ–Pb1–I1ⁱ	153.11(2)
O1–Pb1–I1ⁱⁱ	82.26(11)	O1–Pb1–I1ⁱ	79.20(3)	O1ⁱ–Pb1–I1	79.20(3)

Compound 3

Pb1–O1	2.294(6)	I1–Pb1	3.203(1)	O1–Pb1ⁱ	2.586(4)
Pb1–N1	2.476(5)	Pb1–I1ⁱ	3.604(6)	Pb1–I1ⁱⁱ	3.519(4)
Pb1–O1i	2.586(4)	Pb1–I1	3.203(1)	H1–I1ᵛⁱ	3.148(5)
Pb1–Pb1ⁱ	3.951(1)	O1–C8	1.335(6)	H3–O2ⁱⁱⁱ	2.380(7)
O1–Pb1–N1	69.39(14)	O1i–Pb1–I1	159.57(8)	O1–Pb1–I1	92.27(9)
O1–Pb1–O1ⁱ	72.06(12)	Pb1–O1–Pb1i	107.94(14)	N1–Pb1–I1	80.33(11)
N1–Pb1–O1i	105.17(14)	I1ⁱ–Pb1–I1	110.78(1)	I1ⁱ–Pb1–I1ⁱⁱ	133.41(1)
I1–Pb1–I1ⁱⁱ	81.02(1)				

30 min at room temperature and then filtered. The filtrate was kept at room temperature for two weeks to obtain blown block single crystals of 0.62 g (42%, based on Pb). Calcd. for $C_5H_4I_2NOPb$ (555.09): C, 11.12; H, 0.68; N, 2.47%; found: C, 11.10; H, 0.70; N, 2.50%. IR (cm^{-1}): 3080(w), 1621(w), 1466(s), 1417(m), 1214(s), 1214(s), 1167(m), 831(m), 549(m).

[PbI$_2$(bipyO$_2$)]$_n$ (2). The procedure for **2** was also similar to the synthesis of compound **1** by reactions of bipyO$_2$ (0.19 g, 1.0 mmol), Pb(NO$_3$)$_2$ (0.33 g, 1 mmol) and NaI·2 H$_2$O (0.37 g, 2 mmol) in DMF (15 mL). Yield: 0.21 g (*ca.* 25%, based on Pb). Calcd. for $C_{10}H_8I_2N_2O_2Pb$ (649.18): C, 18.48; H, 1.23; N, 4.31%; found: C, 18.45; H, 1.25; N, 4.30%. IR (cm^{-1}): 3076(w), 1628(w), 1465(m), 1421(s), 1222(s),1205(m), 837(m), 767(m), 583(s).

{[PbI(Dhydql)]·DMF}$_n$ (3). The procedure for **3** was different from the synthesis of compounds **1** and **2**. Hydql (0.19 g, 1.0 mmol), Pb(NO$_3$)$_2$ (0.33 g, 1 mmol) were solved in DMF and 10 drops of 30% NaOH/DMF solution was added and stirred for 30 min. Thereafter, NaI·2 H$_2$O (0.33 g, 3 mmol) was added and stirring continued at 85 °C for 8 h and cooled to room temperature freely and filtered. The filtrate was kept at room temperature for seven days to obtain red block single crystals. Yield: 55% (*ca.* 0.67 g, based on Pb). Calcd. for $C_{12}H_{13}IN_2O_2Pb$ (551.34): C, 26.10, H, 2.35; N, 5.04%; found: C, 26.12, H, 2.36; N, 5.08% IR (cm^{-1}): 3046(w), 1651(w), 1567(m), 1560(s), 1489(m), 1458(s), 1377(s), 1100(m), 821(m), 728(s), 488(s).

X-Ray structure determination

X-Ray data on suitable single crystals of **1–3** were collected at 293(2) K with a Rigaku Weissenbery IP diffractometer using graphite-monochromated Mo Kα radiation ($\lambda = 0.710\ 69$ Å). All three structures were solved by a direct method and refined by full-matrix least-squares techniques on F^2 using SHELXTL-97.[48,49] All non-hydrogen atoms were treated anisotropically. The hydrogen atoms of C–H were generated geometrically. Crystallographic data and structural refinement details for **1–3** are summarized in Table 2. Important bond lengths and angles are given in Table 3.

CCDC Nos. 634298 (**1**), 656622 (**2**) and 659647 (**3**) contain supplementary crystallographic data for this paper. These data can be obtained free of charge at http://www.ccdc.cam.ac.uk/conts/retrieving.html (or from the Cambridge Crystallographic Data Centre (CCDC), 12 Union Road, Cambridge CB2 1EZ, U.K. fax, +44(0)1223-336033; e-mail: deposit@ ccdc.cam.ac.uk).

Acknowledgements

References

1 K. Chondroudis, D. B. Mitzi and P. Brock, *Prog. Inorg. Chem.*, 1999, **48**, 1.
2 D. B. Mitzi, S. Wang, C. A. Field, W. T. A. Harrison and A. M. Guloy, *Nature*, 1994, **369**, 467.
3 D. B. Mitzi, S. Wang, C. A. Chess, C. A. Field and A. M. Gulo, *Science*, 1995, **267**, 1473.
4 S. Wang, D. B. Mitz, C. A. Field and A. M. Guloy, *J. Am. Chem. Soc.*, 1995, **117**, 5297.
5 J. Calabrese, N. L. Jone, R. L Harlow, N. Herron, D. L. Thorn and Y. J. Wang, *J. Am. Chem. Soc.*, 1991, **113**, 2328.
6 N. Mercier, A. L. Barres, M. Giffard, I. Rau, F. Kajzar and B. Sahraoui, *Angew. Chem., Int. Ed.*, 2006, **45**, 2100.
7 H. Krautscheid, F. Vielsack and N. Z. Klaassen, *Z. Anorg. Allg. Chem.*, 1998, **624**, 807.
8 C. Lode and H. Z. Krautscheid, *Z. Anorg. Allg. Chem.*, 2001, **627**, 1454.
9 J. H. Yu, H. B. Jia, L. Y. Pan, Q. X. Yang, T. G. Wang, J. Q. Xu, X. B. Cui, Y. J. Liu, Y. Z Li, C. H. Lin and T. H. Ma, *J. Solid State Chem.*, 2003, **175**, 152.
10 D. B. Mitzi and P. Brock, *Inorg. Chem.*, 2001, **40**, 2096.
11 X. H. Zhu, N. Mercier, P. Frere, P. Blanchard, J. Roncali, M. Allain, C. Pasquier and A. Riou, *Inorg. Chem.*, 2003, **42**, 5330.
12 X. H. Zhu, N. Mercier, M. Allain, P. Prere, P. Blanchard, J. Roncali, C. Pasquier and A. J. Riou, *J. Solid State Chem.*, 2004, **177**, 1067.
13 Z. J. Zhang, S. C. Xiang, Y. F. Zhang, A. Q. Wu, L. Z. Cai, G. C. Guo and J. S. Huang, *Inorg. Chem.*, 2006, **45**, 1972.
14 D. B. Mitzi, C. A. Field, Z. Schlesinger and R. B. Laibowitz, *J. Solid State Chem.*, 1995, **114**, 159.
15 T. Ishihara, *Optical Properties of Low-Dimensional Materials*, ed. T. Ogawa and Y. Kanemitsu, World Scientific, Singapore, 1995, ch. 6.
16 S. Wang, D. B. Mitzi, C. A. Feild and A. M. Guloy, *J. Am. Chem. Soc.*, 1995, **117**, 5297.
17 S. K. Dutta and M. W. Perkovic, *Inorg. Chem.*, 2002, **41**, 6938.
18 B. H. Hamilton, K. A. Kelly, K. A. Kelly, T. A. Wagler, M. P. Espe and C. J. Ziegler, *Inorg. Chem.*, 2004, **43**, 50.
19 Y. J. Shi, G. Q. Jiang, Y. H. Zhu and X. Z. You, *Appl. Organomet. Chem.*, 2004, **18**, 89.
20 J. M. Harrowfield, H. Miyamae, B. W. Skelton, A. A. Soudi and A. H. White, *Aust. J. Chem.*, 1996, **49**, 1121.
21 V. N. Kokozay, V. R. Polyakov and Y. A. Simonov, *J. Coord. Chem.*, 1993, **28**, 191.
22 L. Y. Kong, Z. H. Zhang, T. Okamura, M. J. Fei, W. Y. Sun and N. Ueyama, *Chem. Lett.*, 2004, **33**, 1572.
23 H. G. Zhu, Y. Xu, Z. Yu, Q. J. Wu, H. K. Fun and X. Z. You, *Polyhedron*, 1999, **18**, 3491.
24 X. T. Chen, Z. L. Xue and X. Z. You, *Inorg. Chem. Commun.*, 2002, **5**, 1090.
25 M. Sarı, S. Surmuş, O. Atakol, I. Svoboda and H. Fuess, *Acta Crystqllogr., Sect. E*, 2001, **57**, m201.
26 (*a*) C. J. Horn, A. J. Blake, N. R. Champness, A. Garau, V. Lippolis, C. Wilson and M. Schroder, *Chem. Commun.*, 2003, 312; (*b*) S. S. Batsanov, *Russ. J. Inorg. Chem.*, 1991, **36**, 1694.
27 G. Barbera, C. Vinas, F. Teixidor, G. M. Rosair and A. J. Welch, *J. Chem. Soc., Dalton Trans.*, 2002, 3647.
28 O. Y. Vassilyeva, V. N. Kokozay, N. I. Zhukova and L. A. Kovbasyuk, *Polyhedron*, 1997, **16**, 263.
29 S. Wang, D. B. Mitzi, C. A. Field and A. Guloy, *J. Am. Chem. Soc.*, 1995, **117**, 5297.
30 N. Mercier, S. Poiroux, A. Riou and P. Batail, *Inorg. Chem.*, 2004, **43**, 8361.
31 N. Mercier, *CrystEngComm*, 2005, **7**, 429.
32 Z. J. Zhang, G. C. Guo, G. Xu, M. L. Fu, J. P. Zou and J. S. Huang, *Inorg. Chem.*, 2006, **45**, 10028.
33 D. B. Mitzi, D. R. Medeiros and P. R. L. Malenfant, *Inorg. Chem.*, 2002, **41**, 2134.
34 Y. J. Shi, Y. Xu, Y. Zhang, B. Huang, D. R. Zhu, C. M. Jin, H. G. Zhu, Z. Yu, X. T. Chen and X. Z. You, *Chem. Lett.*, 2001, 678.
35 P. Hohenberg and W. Kohn, *Phys. Rev.*, 1964, **136**, B864.
36 W. Kohn and L. Sham, *Phys. Rev.*, 1965, **140**, A1133.
37 P. H. Lin, S. L. Chang and Z. P. Guo, *J. Yanbian Univ. (Nat. Sci.)*, 2004, **30**, 274.
38 G. Kotujm, *Reflectance Spectroscopy*, Springer-Verlag, New York, 1969.

39 W. W. Wendlandt and H. G. Hencht, *Reflectance Spectroscopy*, Interscience, New York, 1966.

40 S. P. Tandon and J. P. Gupta, *Phys. Status Solidi*, 1970, **38**, 363.

41 T. J. McCarthy, T. A. Tanzer and M. G. Kanatzidis, *J. Am. Chem. Soc.*, 1995, **117**, 1294.

42 G. Cao, L. K. Rabenberg, C. M. Nunn and T. E. Mallouk, *Chem. Mater.*, 1991, **3**, 149.

43 Y. Y. Niu, Y. L. Song, H. W. Hou and Y. Zhu Hou, *Inorg. Chem.*, 2005, **44**, 2553.

44 M. S. Bahae, A. A. Said, T. H. Wei, D. J. Hagan and E. W. Van Stryland, *IEEE J. Quantum Electron.*, 1990, **26**, 760.

45 H. Krautscheid, J. F. Lekieffre and J. Besinger, *Z. Anorg. Allg. Chem.*, 1996, **622**, 1781.

46 P. G. Simpon, A. Vinciguerra and J. V. Quagliano, *Inorg. Chem.*, 1963, **2**, 282.

47 (*a*) W. W. Wendlandt and H. G. Hecht, *Reflectance Spectroscopy*, Interscience Publishers, New York, 1966; (*b*) G. Kotiim, *Reflectance Spectroscopy*, Springer-Verlag, New York, 1969; (*c*) O. Schevciw and W. B. White, *Mater. Res. Bull.*, 1983, **18**, 1059.

48 SADABS, *Bruker Smart and Bruker SHELXL Package*, Bruker AXS GmhH, 1998.

49 G. M. Sheldrick, *SHELX97, Program for Crystal Structure Refinement*. University of Gottingen, Germany, 1997.